Supporting Information

Brown et al. 10.1073/pnas.1109038108

SI Methods

Subject Demographics and Neuropsychological Testing. Subjects were recruited from the University of California (Los Angeles) Memory Clinic at the Semel Institute for Neuroscience and Human Behavior to participate in an ongoing, comprehensive study of aging and dementia. Subjects performed a diagnostic evaluation that consisted of physical and neurological examinations, a medical history assessment, genotyping for apolipoprotein E (*APOE*), and neuropsychological testing. We excluded subjects on the basis of left-handedness, a history of neurological or psychiatric disorders, medication affecting cognition, alcohol or substance abuse, head trauma, epilepsy, arterial hypertension, or cardiovascular disease. Blood was drawn from each subject and genotyped for *APOE* (1).

The study included 30 *APOE*-4 noncarriers (average age, 63.8 ± 8.3 y; range, 45–76; 20 female; education, 16.7 ± 1.8 y; 21 with family history of dementia) and 25 *APOE*-4 carriers (average age, 60.8 ± 9.7 y; range, 43–78; 12 female; 21 3/4s, 4 4/4s; education, 17.5 ± 3.3 y; 16 with family history of dementia).

Subjects scored ≥27 on the mini-mental state examination (MMSE) with the exception of one subject who scored 26 but fell within the normal range on the remaining neuropsychological tests; analyses that excluded that subject found equivalent results. Forty-three of the 55 subjects were tested for subjective memory complaints, using the Memory Functioning Questionnaire (2). Scores were in the age-typical range and no significant between-group differences were found in frequency of forgetting (*APOE*-4, 157 ± 27; *APOE*-4 NC, 164 ±27), seriousness of forgetting (87 ± 25, 90 ±20), retrospective functioning (14.7 ± 4, 14.8 ±4.4), or mnemonics use (18.9 ± 8.6, 20.5 ± 8.4) (all $P > 0.2$).

The neuropsychological battery included (*i*) Wechsler memory scale, logical memory delayed recall portion (WMS LM delay); (*ii*) Buschke–Fuld selective reminding test (consistent long-term retrieval section, Buschke CLTR); (*iii*) Rey–Osterrith Complex Figure, delayed recall (Rey-O delay); (*iv*) Wechsler memory scale, verbal paired associations II (WMS VP); and (*v*) Wechsler Adult Intelligence Scale III digit span (WAIS digit span).

Diffusion Tensor Imaging (DTI) Preprocessing and Tractography. Scans were processed using programs from the FMRIB Software Library (FSL; www.fmrib.ox.ac.uk/fsl/). Diffusion tensors were then estimated at each voxel and fractional anisotropy (FA) images were created. Raw DTI images were first corrected for eddy current distortions using a 12-df affine registration to the first B0 volume.

Regional masks were transformed to each subject's diffusion space using a multistage registration process. First, the high-resolution structural image magnetization-prepared rapid gradient echo (MP-RAGE) was skull stripped using FSL's Brain Extraction Tool (BET). Next, the FA image was affine registered to the MP-RAGE using 12 degrees of freedom and a mutual information cost function using FSL's Linear Image Registration Tool (FLIRT). The MP-RAGE was then affine registered to the MNI152 brain using 12 df and a correlation ratio cost function. These two transformation matrices were multiplied and inverted to obtain the standard space-to-diffusion space transformation matrix.

The probability distribution of fiber direction(s) in each voxel was estimated using BEDPOSTX, configured to allow for up to two crossing fibers within each voxel (3). The dyads for the first and second vectors of diffusion direction within each voxel were used for tractography. Typically these dyads are used as the input to a probabilistic tractography program. However, probabilistic estimates of structural connectivity can be difficult to interpret when building a connectivity matrix. For this reason, we used these dyad vectors as the input for deterministic tractography, using the fiber assignment by continuous tracking (FACT) algorithm in Diffusion Toolkit (ref. 4 and http://trackvis.org/dtk). Whole brain tractography was carried out, propagating fibers from each voxel with a maximum turn angle of 50°. Fibers were smoothed using a spline filter and all fibers <5 mm were excluded. To control for false positives, any region–region pair with less than three connecting fibers had its connection strength set to 0. A fiber was defined as connecting two regions if one fiber endpoint lay within one region and the other endpoint lay within the other region.

Because the regions from the Harvard Oxford Atlas varied in volume (450–46,800 mm^3), the fiber counts had to be adjusted for the unequal number of seed voxels in each region. The fiber connectivity metric between two regions was therefore scaled by the mean of the two regions' volumes. This step had the additional benefit of correcting for individual variations in brain size with finer accuracy than can be achieved with a global correction for brain volume. Connectivity matrices resulted and ranged between 16.1% and 23.7% of regions connected. These individual variations in connection "density" had no significant relationship to any neuropsychological measure and decreased with age at nearly equal rates in the *APOE*-4 carriers and noncarriers.

Network Metrics. Given a weighted connectivity matrix, strength was calculated as the total weight of connections to a given node. To calculate cost, for each region–region connection the product of fiber count (i.e., connection weight, w_{ij}), average fiber length (l_{ij}), and average fiber FA (fa_{ij}) and was taken. The sum of all region–region costs was computed to derive the total network cost:

$$\sum w_{ij}\bar{l}_{ij}fa_{ij}.$$

For each node, the subgraph was defined as the subset of connections between the node and its first-degree neighbors. The clustering coefficient for a node was calculated as the ratio of the number of actual connections among the neighbors in the subgraph to the number of possible connections, scaled by the edge weights.

To calculate path lengths within the networks, the distance matrix was first defined. Distance was defined in two parts: First, the inverse of fiber density between two regions was calculated, with the rationale that a denser connection enables more communication and is equivalent to a shorter distance. Second, this distance was scaled by the actual average length of fibers connecting the regions. This distance scaling step allowed the quantification of network path lengths in terms of true physical distance. Shortest paths were determined between all pairs of nodes (e.g., node A and node B) in the network by finding the shortest distance between nodes A and B using Djikstra's algorithm, which finds all possible paths between A and B that travel through a unique, nonlooping set of other nodes. These paths are then sorted by distance, where distance is the product of the connection weight for each jump between nodes along the path and the anatomical distance between those nodes. Characteristic path length measured the average shortest path length in the network.

Small worldness for a network was calculated with respect to a set of equivalent "null" random networks that have the same sum of weights as the real network but have been randomly re-

wired. For each subject's structural network, we calculated 1,000 random networks for comparison. Normalized clustering coefficient was calculated as the ratio of the clustering coefficient from the real network to the average clustering coefficient of the 1,000 random networks. Normalized characteristic path length was calculated in the same fashion. Small worldness was quantified as the ratio of normalized clustering coefficient and normalized characteristic path length.

Graph Theory Formulas. Network measures were calculated with the Brain Connectivity Toolbox, which is based on formulas described elsewhere (5). Briefly, strength was calculated as $k_i = \sum w_{ij}$, where w_{ij} is the weight between nodes i and j.

Clustering coefficient was calculated as $C = \frac{1}{n}\sum \frac{\sum (w_{ij} w_{ih} w_{jh})^{1/3}}{k_i(k_i - 1)}$, where all w are weights and k is the number of nodes in the local, first-degree neighborhood.

Characteristic path length was calculated as $L = \frac{1}{n}\sum \frac{\sum d_{ij}}{n-1}$, where d_{ij} is the path weight between any nodes i and j in the network that pass through the specified node. The average of these path weights is the average path weight for the node. The average of the average path weights for each node is the characteristic path length.

Normalized clustering coefficient (CC) (λ) was calculated as $\lambda = \frac{\mathrm{CC}_{\mathrm{real}}}{\mathrm{CC}_{\mathrm{random}}}$, where $\mathrm{CC}_{\mathrm{random}}$ is the mean CC from the 1,000 random networks.

Normalized characteristic path length (CPL) (γ) was then $\gamma = \frac{\mathrm{CPL}_{\mathrm{real}}}{\mathrm{CPL}_{\mathrm{random}}}$, where again $\mathrm{CPL}_{\mathrm{random}}$ is the mean from 1,000 random networks.

Finally, small worldness (σ) was the ratio $\sigma = \frac{\lambda}{\gamma}$.

A small world network has no isolated nodes, $\lambda >> 1$, $\gamma \cong 1$, and $\sigma > 1.2$.

Graph Visualization. Network graphs were rendered using matplotlib (http://matplotlib.sourceforge.net) and networkX (http://networkx.lanl.gov).

Statistics. Three regression models were tested for mean clustering coefficient. Regression model 1, including only main effects, showed significant main effects of genotype ($P = 0.02$), sex ($P = 0.003$), and age ($P = 0.004$ or $P < 0.01$) on mean clustering coefficient and was significant overall [$f(49, 5) = 27.98$, $P = 2.79 \times 10^{-13}$]. Model 2, adding the age × genotype, showed a significant genotype × age interaction ($P = 0.04$) and was also significant overall [$f(48, 6) = 25.83$, $P = 1.82 \times 10^{-13}$]. Model 3, the model selected by stepwise regression, included genotype, sex, and genotype × age interaction. There was a significant age × genotype interaction ($P = 0.0005$) and the model was significant overall [$f(49, 5) = 31.17$, $P = 4.01 \times 10^{-14}$]. This model was the most accurate predictor of mean clustering coefficient.

The same three models were tested for mean cortical thickness, Rey-O delay, and WMS LM delay: model 1, mean cortical thickness [$f(50, 4) = 17.43$, $P = 5.16 \times 10^{-9}$], Rey-O delay [$f(51, 3) = 1.63$, $P = 0.19$], WMS LM delay [$f(51, 3) = 3.65$, $P = 0.02$]; model 2, mean cortical thickness [$f(49, 5) = 15.02$, $P = 6.18 \times 10^{-9}$], Rey-O delay [$f(50, 4) = 2.63$, $P = 0.044$], WMS LM delay [$f(50, 4) = 3$, $P = 0.03$]; and model 3, mean cortical thickness [$f(50, 4) = 19.06$, $P = 1.41 \times 10^{-9}$], Rey-O delay [$f(51, 3) = 3.58$, $P = 0.02$], WMS LM delay [$f(51, 3) = 3.89$, $P = 0.014$]. In every case, model 3 had the smallest P value.

Interpretability of the genotype × age interaction on regional clustering coefficient was also assessed by examining the partial correlation between age and regional clustering separately for *APOE*-4 carriers and noncarriers after controlling for the effect of sex, scanner, and total network cost.

1. Wenham PR, Price WH, Blandell G (1991) Apolipoprotein E genotyping by one-stage PCR. *Lancet* 337:1158–1159.
2. Gilewski MJ, Zelinski EM, Schaie KW (1990) The Memory Functioning Questionnaire for assessment of memory complaints in adulthood and old age. *Psychol Aging* 5:482–490.
3. Behrens TEJ, Berg HJ, Jbabdi S, Rushworth MFS, Woolrich MW (2007) Probabilistic diffusion tractography with multiple fibre orientations: What can we gain? *Neuroimage* 34:144–155.
4. Mori S, van Zijl PCM (2002) Fiber tracking: Principles and strategies - a technical review. *NMR Biomed* 15:468–480.
5. Rubinov M, Sporns O (2010) Complex network measures of brain connectivity: Uses and interpretations. *Neuroimage* 52:1059–1069.

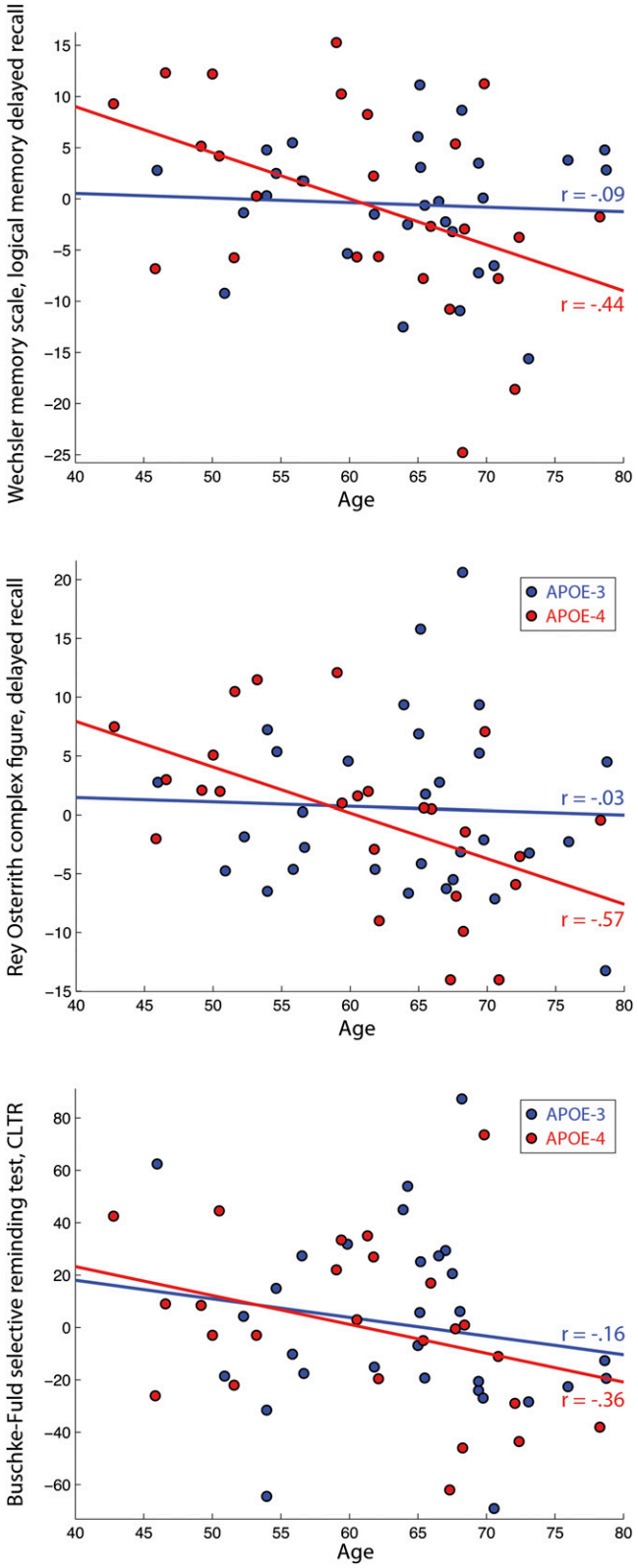

Fig. S1. Wechsler memory scale (logical memory delayed recall portion, WMS LM delay), Rey–Osterrith Complex Figure (delayed recall, Rey-O delay), and Buschke–Fuld selective reminding test (consistent long-term retrieval section, Buschke CLTR) residuals based on partial correlations with age plotted for *APOE*-4 noncarriers (*APOE*-3, blue) and *APOE*-4 carriers (red). Partial correlations controlled for sex. Both WMS LM delay and Rey-O delay had a significant interaction between *APOE* genotypes ($P < 0.05$).

Table S1. Top 12 regions with highest combined rank for strength, betweenness centrality, and regional short path length for *APOE*-4 noncarriers (*APOE*-4 NC) and *APOE*-4 carriers

APOE-4 NC	*APOE*-4
Left angular gyrus	Left insular cortex
Left precuneus	Right insular cortex
Left superior temporal gyrus (posterior)	Left posterior cingulate
Left intracalcarine cortex	Right cuneal cortex
Right supramarginal gyrus (posterior)	Left temporal pole
Left posterior cingulate	Right temporal pole
Left insular cortex	Right intracalcarine cortex
Left supramarginal gyrus (posterior)	Right posterior cingulate
Right insular cortex	Right precuneus
Left lateral occipital cortex (superior)	Left supramarginal gyrus (posterior)
Right intracalcarine cortex	Right frontal orbital cortex
Left middle temporal gyrus (temporooccipital)	Right lingual gyrus

Table S2. Regions that show a significant interaction in the selected regression model

Region	*APOE*-4 partial correlation with age, *r*	Associated *P* value	*APOE*-4 NC partial correlation with age, *r*	Associated *P* value	Comparison of correlation coefficients, *P* value
R precentral gyrus	−0.5	0.017	−0.2	0.33	0.03
R inferior temporal gyrus, anterior	−0.58	0.005	−0.13	0.52	0.01
L inferior temporal gyrus, posterior	−0.65	0.0009	0	0.97	0.005
L supramarginal gyrus, posterior	−0.54	0.009	−0.35	0.07	0.02
L subcallosal cortex	−0.54	0.009	−0.06	0.77	0.02
R anterior cingulate gyrus	−0.48	0.02	0.02	0.9	0.03
R precuneus cortex	−0.64	0.001	−0.13	0.53	0.006
L frontal orbital cortex	−0.5	0.02	−0.17	0.4	0.03

In all cases, the partial correlation of regional clustering and age is significantly negative for *APOE*-4 carriers ($P < 0.05$) and nonsignificant for *APOE*-4 noncarriers ($P > 0.05$), and the partial correlation coefficients are significantly different between groups ($P < 0.05$). L, left; R, right.